Radial pattern of nuclear decay processes

W. Iskra,[1,2] M. Müller,[1] and I. Rotter[1,3]
[1] *Forschungszentrum Rossendorf, Institut für Kern- und Hadronenphysik, D-01314 Dresden, Germany*
[2] *Soltan Institute for Nuclear Studies, PL-00-681 Warszawa, Poland*
[3] *Technische Universität Dresden, Institut für Theoretische Physik, D-01062 Dresden, Germany*
(Received 18 May 1994)

At high level density of nuclear states, a separation of different time scales is observed (trapping effect). We calculate the radial profile of partial widths in the framework of the continuum shell model for some 1^- resonances with $2p$-$2h$ nuclear structure in ^{16}O as a function of the coupling strength to the continuum. A correlation between the lifetime of a nuclear state and the radial profile of the corresponding decay process is observed. We conclude from our numerical results that the trapping effect creates structures in space and time characterized by a small radial extension and a short lifetime.

PACS number(s): 24.30.−v, 21.10.Tg, 21.60.Cs, 24.60.Lz

I. INTRODUCTION

Recently, the properties of open quantum systems are investigated in the framework of different models [1–12]. In most cases studied, the number N of resonance states is much larger than the number K of open decay channels. One of the results obtained is the *trapping effect* which appears if the average width $\bar{\Gamma}$ of the resonance states is of the same order of magnitude as their average distance $\bar{D}$. In this case, a redistribution takes place inside the nucleus which results in the formation of K short-lived resonance states ("broad states") together with N-K long-lived ones ("narrow states"). The time scales of both types of states are well separated from each other.

The trapping effect is shown to occur in realistic many-body quantum systems such as nuclei. Here, at low level density, the nuclear spectroscopic properties are relevant, while at higher level density, the properties of nuclei are described well by the unified theory of nuclear reactions where the open decay channels are relevant. It is exactly this transition which is described by the redistribution taking place inside the nucleus at the critical degree $\bar{\Gamma}/\bar{D} \approx 1$ of resonance overlapping [4]. Further, in strong-absorption cases, a proper statistical theory of the reaction amplitude yields such a broad distribution of resonance pole widths and strengths that individual pole terms giving rise to intermediate structure resonances in the cross section appear with appreciable probability [13].

Further, the trapping effect explains the different properties of resonances observed in light and heavy nuclei. While the lifetimes of the resonances in light nuclei are of the order of magnitude of the collision time between nucleons (apart from selection rules), the resonances in heavy nuclei are very long-lived. They are strongly mixed in the basic shell-model wave functions which corresponds to the original definition of the compound nucleus given by Bohr [14].

The trapping effect is the result of the interference between a certain number N of overlapping resonances. Thus, one could expect that the radial extensions of the broad and narrow states are of comparable size. On the other hand, the lifetimes of the long-lived and short-lived states differ strongly from each other so that there exists, maybe, a correlation with the radial extension of the nucleus.

There are two different possibilities for such a correlation, which both have their own justification. One could imagine that the long-lived states have a narrower radial extension than the short-lived ones with the consequence that they are screened from the continuum. This might be the reason for their long lifetimes. Another idea is the interpretation of the trapping effect as the formation of *structures in space and time* by self-organization [15]. In such a case, the radial extension of the short-lived states is expected to be smaller than that of the long-lived ones. In this case, the broad states appear to be localized in both time and space while the long-lived states are spread over a larger extension in time as well as in space.

The purpose of our investigation is to clarify whether there is any relation between the lifetimes of resonance states and their radial extension. In our calculations, the radial extension of a state is *not* determined directly. We calculate, instead, the radial pattern of the partial width amplitudes, i.e., of the area at which the emission of the particles from the resonance states takes place. The partial width amplitudes vanish at the center of the nuclear states where the channel wave functions are small, and are sensitive to the radius of the resonance state where its wave function vanishes. The results obtained show clearly a correlation between lifetime and radius of different states.

II. MODEL CALCULATIONS

The radial profile of the partial width amplitudes is studied in the framework of the continuum shell model in line with the method described in [16].

In the continuum shell model, the Schrödinger equation

$$(H - E)\Psi = 0 \tag{1}$$

is solved with an ansatz containing both bound and un-

bound states. The total function space is subdivided, by using the projector operator technique, into the two orthogonal subspaces P and Q under the condition $P+Q=1$. The subspace Q contains the many-body states of A nucleons formed by the antisymmetrized products of the wave functions of the single-particle bound states and of the single-particle resonance wave functions up to some cutoff radius. Therefore, the structural part in the continuum shell model is the same as in the standard shell-model approaches. The eigenstates Φ_R^{SM} of the Q-projected Hamiltonian H_{QQ} are called [17] "quasibound states embedded in the continuum" (QBSEC). These QBSEC's differ from the "bound states embedded in the continuum" (BSEC) introduced by Mahaux and Weidenmüller [18] by the contribution of the single-particle resonances from the interior of the nucleus ("cutoff procedure"). The subspace P contains the many-body states with $A-1$ nucleons in bound orbits and one nucleon in a scattering state as well as the part of the single-particle resonance wave functions beyond the cutoff radius.

Using the cutoff procedure for single-particle resonances, it is possible to identify the matrix elements

$$\begin{aligned}\tilde{\gamma}_{Rc} &= (2\pi)^{1/2}\langle\chi_E^c|V|\tilde{\Omega}_R\rangle \\ &= (2\pi)^{1/2}\langle\xi_E^c|V|\tilde{\Phi}_R\rangle,\end{aligned} \tag{2}$$

with the amplitudes of the partial widths [19]. Here, the $\tilde{\Phi}_R$ are the eigenfunctions of the non-Hermitean operator

$$H_{QQ}^{\text{eff}} = H_{QQ} + H_{QP}\, G_P^{(+)}\, H_{PQ}, \tag{3}$$

where $G_P^{(+)}$ is the Green function in the P subspace and

$$H = H_0 + V \tag{4}$$

contains the central potential H_0 as well as the two-particle residual interaction V. Using the projector operator formalism, the Hamiltonian consists of four parts

$$H = H_{QQ} + H_{QP} + H_{PQ} + H_{PP} \tag{5}$$

where $H_{PQ} \equiv PHQ$ and so on. It is $\tilde{\Phi}_R = \sum_{R'} a_{RR'}\ \Phi_{R'}^{SM}$ with complex coefficients $a_{RR'}$. The Φ_R^{SM} are the eigenfunctions of H_{QQ} (shell-model wave functions) which are represented as $\Phi_R^{SM} = \sum_{R'} b_{RR'}\Phi_{R'}^0$ where the Φ_R^0 are the Slater determinants belonging to H_0. The functions ξ_E^c are solutions of the coupled-channel equations $(H_{PP}-E)\xi_E^c = 0$ while the χ_E^c are the channel wave functions (wave functions t of the target (or residual) nucleus in a certain state and one unbound nucleon). The functions

$$\tilde{\Omega}_R = (Q + G_P^{(+)}\, H_{PQ})\ \tilde{\Phi}_R \tag{6}$$

are the wave functions of the resonance states R. The details of the model can be found in [17, 4].

In the second quantization method, the two-body residual interaction reads as follows:

$$V = \frac{1}{2}\sum_{ijkl} V_{ijkl} : a_i^+ a_j^+ a_l a_k : \tag{7}$$

where $\{i\} \equiv \binom{n_i}{\varepsilon_i} l_i j_i m_i \tau_i$ with n_i and ε_i for a bound and unbound particle i, respectively. The V_{ijkl} are defined as

$$V_{ijkl} = \langle\Phi_i(1)\Phi_j(2)|V(\vec{r}_1,\vec{r}_2)|\Phi_k(1)\Phi_l(2)\rangle \tag{8}$$

where Φ_i stands for the one-particle wave function $\frac{1}{r}Y_{l_i j_i}\chi_{\tau_i}\phi_i(r)$. In our calculations, we use a zero-range residual interaction with spin exchange term

$$V(\vec{r}_1,\vec{r}_2) = V_0(a + bP_{12}^{\sigma})\delta(\vec{r}_1 - \vec{r}_2)\ . \tag{9}$$

According to the method used in [16], the radial profile of the amplitudes of the partial widths is calculated from

$$\tilde{\gamma}_{Rc}^r = (2\pi)^{1/2}\langle\xi_E^c|V\delta(r-r')|\tilde{\Phi}_R\rangle \tag{10}$$

where $\delta(r-r')$ is the Dirac delta function. An integration over the radius variable r' in the matrix elements gives us the r-dependent characteristics. Here, r is the radial coordinate of the particle in the continuum (in the outgoing channel).

Let us consider the expression (10) for the $\tilde{\gamma}_{Rc}^r$ in detail. Using the residual interaction (9), Eq. (10) reads

$$\begin{aligned}\tilde{\gamma}_{Rc}^r = \left(\frac{\pi}{2}\right)^{1/2} V_0 \sum_{iklj'} Z_{i'j'k'l'}\ (t|a_i^+ a_l a_k|\tilde{\Phi}_R\rangle \\ \cdot\ \frac{1}{r^2}\ \phi_i(r)\phi_k(r)\phi_l(r)\xi_{j',E}^t(r)\ .\end{aligned} \tag{11}$$

Here, $\{i\},\{k\},\{l\}$ denote the quantum numbers of bound particles while $\{j\}$ stands for those of the unbound particle. The $\{i'\},\{k'\},\{l'\},\{j'\}$ contain all the quantum numbers of the $\{i\},\{k\},\{l\}$, $\{j\}$ but n_i, n_k, n_l, and ε_j, respectively. The $Z_{i'j'k'l'}$ are geometrical factors containing the Clebsch-Gordon-coefficents while the $\xi_{j',E}^t(r) = (t|\xi_E^c\rangle$ are the one-particle channel wave functions projected onto a particular (ground or exited) state $|t)$ of the residual nucleus. They depend on the radial coordinate r and on the quantum numbers $\{j'\}$. It is $\tilde{\Phi}_R = \sum a_{RR'}\ b_{R'R''}\ \Phi_{R''}^0$ where the Φ_R^0 are the Slater determinants of the system with A particles. The target wave functions are represented as $t = \sum_i b_i t_i^0$ where the t_i^0 are the Slater determinants of the system with $A-1$ particles.

The calculations are performed for different values

$$\begin{aligned}W^{\text{ex}} &= \langle\Phi_{R'}^{SM}|H_{QP}G_P^{(+)}H_{PQ}|\Phi_R^{SM}\rangle \\ &= \langle\Phi_{R'}^{SM}|V^{\text{ex}}G_P^{(+)}V^{\text{ex}}|\Phi_R^{SM}\rangle\end{aligned} \tag{12}$$

of the mixing of two resonance states via the continuum of decay channels ("external mixing"). For this purpose, the external part $V^{\text{ex}} = \alpha^{\text{ex}}\ V$ of the interaction in H_{PQ}, H_{QP}, and H_{PP} is varied by means of varying the parameter α^{ex}. The internal part $V^{\text{in}} = \alpha^{\text{in}}\ V$ of the interaction between bound states appearing in H_{QQ} remains constant in our calculations ($\alpha^{\text{in}} = 1$). By varying the external mixing W^{ex}, we change effectively the average degree $\bar{\Gamma}/\bar{D}$ of overlapping of the resonances (Table I).

TABLE I. The main characteristics of the resonance states.

α^{ex}	$\bar{\Gamma}/\bar{D}$	$\tilde{\Gamma}_1$/MeV	$\tilde{\Gamma}_2$/MeV	$\sum_{R=3}^{70}\tilde{\Gamma}_R^{tr}$/MeV	$\chi^2(\tilde{\Gamma}^{tr})$/MeV[a]
Protons					
0.2	0.005	0.01	0.005	0.049	6.5E-05
1.5	0.325	0.66	0.34	2.9	3.4E-03
2.5	0.891	2.4	1.7	6.6	3.8E-02
4	2.212	10.3	9.6	6.7	1.4E-02
8	5.103	43.9	37.2	14.3	2.2E-01
Neutrons					
0.2	0.006	0.01	0.005	0.049	6.5E-05
1.5	0.322	0.71	0.53	2.6	3.3E-03
2.5	0.881	2.8	2.6	5.2	1.8E-02
4	2.187	10.3	10.0	6.0	8.4E-03
8	5.419	43.2	37.6	14.5	2.3E-01

[a] $\chi^2(\tilde{\Gamma}^{tr}) = \overline{(\tilde{\Gamma}_R^{tr} - \tilde{\Gamma}_R^{tr})^2}$.

III. RESULTS

Some typical results of our calculations are shown in Figs. 1 and 2. We have chosen a configuration space of $N = 70$ states 1^- of ^{16}O with $2p$-$2h$ nuclear structure and the $1s$, $1p_{3/2}$, $1p_{1/2}$, $2s$, and $1d_{5/2}$ shells. The number of open decay channels is $K = 2$, which are either the two proton channels $^{15}N_{1/2^-} + p$ and $^{15}N_{3/2^-} + p$ (Fig. 2), or the two neutron channels $^{15}O_{1/2^-} + n$ and $^{15}O_{3/2^-} + n$ (Fig. 1). The energy of the system is $E = 34$ MeV. The inelastic channel opens at $E = 6.30$ MeV in the proton decay and at $E = 6.15$ MeV in the neutron decay, i.e., there are no threshold effects at the energy considered [12]. The parameters of the Woods-Saxon potential for neutrons as well as for protons are taken from calculations describing proton scattering on ^{15}N [12, 17]. The Coulomb potential corresponds to a homogeneous charged sphere of radius $1.25\,(A-1)^{1/3} = 3.08$ fm. The parameters of the residual interaction V are the same as in [12].

The calculations are performed for $\alpha^{ex} = 0.2$ up to $\alpha^{ex} = 8$. The trapping effect appears at $\alpha_{cr}^{ex} \approx 2.6$ where $\bar{\Gamma}/\bar{D} \approx 1$ (see Table I) [12], i.e., our calculations at $\alpha^{ex} = 0.2$ are well below the critical region α_{cr}^{ex} while those with $\alpha^{ex} = 8$ are beyond it. The widths $\tilde{\Gamma}_R$ of the states are given in Table I. In each case, $R = 1$, 2 are the two states with the largest widths (second and third columns). The sum of the widhts of the remaining 68 states as well as its averaged squared deviation χ^2 are given in the two last columns. Just above the critical point α_{cr}^{ex}, where the two broad states separate from the other resonances, the widths of most of the trapped modes decrease. Therefore, the χ^2 show a minimum in this region of α^{ex}.

The radial profiles $\{\tilde{\gamma}_{Rc}^r\}$ are complex because they contain the complex wave functions $\tilde{\Phi}_R$ and $\xi_{j',E}^t(r)$. In Figs. 1(a)–1(h), $\mathrm{Re}\{\tilde{\gamma}_{Rc}^r\}$ for the inelastic neutron channel is drawn for $\alpha^{ex} = 0.2$ to 8. In Fig. 2, $\mathrm{Re}\{\tilde{\gamma}_{Rc}^r\}$ as well as $\mathrm{Im}\{\tilde{\gamma}_{Rc}^r\}$ are shown for both channels c_1 [Figs. 2(a,b,e,f)] and c_2 [Figs. 2(c,d,g,h)] in the case of proton decay and for $\alpha^{ex} = 0.2$ and 8. In any case, the $\tilde{\gamma}_{Rc}^r$ for the two states $R = 1$, 2 with the largest widths are represented by dashed lines while the $\tilde{\gamma}_{Rc}^r$ of all the other states $R = 3, ..., 70$ are shown by dots at the radii r for which the calculations are performed. The solid curves in Fig. 1 are drawn for a typical trapped state.

The results of our calculations show the following: With increasing α^{ex} the amplitudes $\tilde{\gamma}_{Rc}^r$ increase for all states. Further, the transition matrix elements for the broad states get dominant peaks at small radii if the coupling strength increases. That means, the fast decays take place mostly in the inner part of the nucleus. In contrast to that, the decay of the trapped states is distributed over the whole nucleus.

In other words, most nucleons which appear quickly from the short-lived resonances, are emitted in the internal region. The nucleons emitted in the surface region (2 to 3 fm) arise from both, the long-lived and the short-lived states. These results are independent of the charge of the emitted particle [compare Figs. 1(a), 1(h) and 2(c), 2(d)]. They are well expressed for the calculations with $\alpha^{ex} > \alpha_{cr}^{ex}$ where the widths of the two broadest resonances are well separated from those of the other 68 resonances.

It should be underlined here that the $\{\tilde{\gamma}_{Rc}^r\}$ of the two broadest resonances $R = 1, 2$ do not change their sign as a function of r in our calculations for α^{ex} above the critical point. After integrating over r, one gets therefore large values for the amplitudes of the partial widths $\tilde{\gamma}_{Rc} = \int \tilde{\gamma}_{Rc}^r\, dr$.

IV. DISCUSSION

The results obtained are unequivocal from the numerical point of view. Nevertheless, a discussion of them is necessary in order to understand their physical meaning.

As stated in the Introduction, the radial extension of

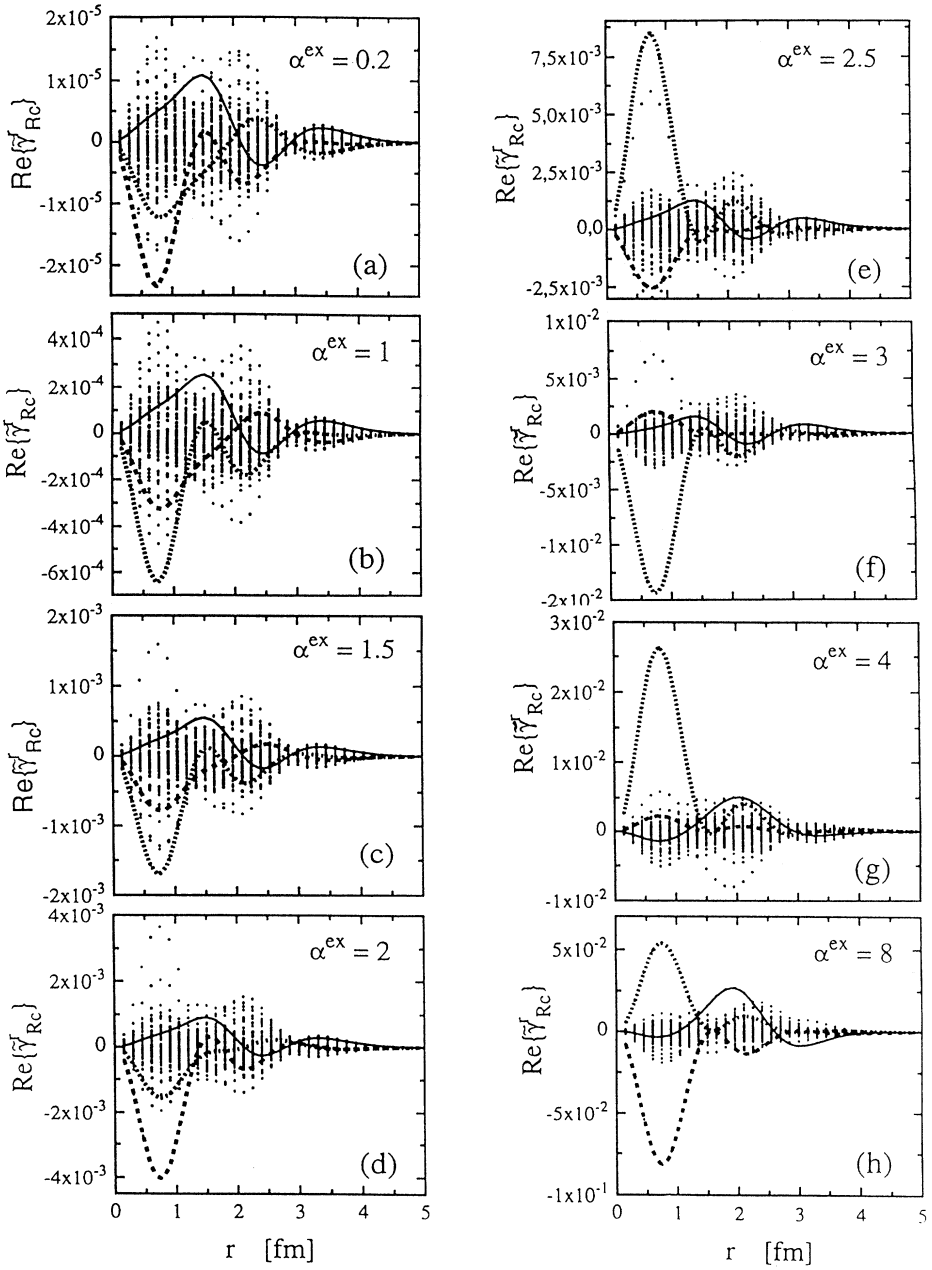

FIG. 1. $\mathrm{Re}\{\tilde{\gamma}^r_{Rc}\}$ for the inelastic neutron channel c_2 and for $\alpha^{ex} = 0.2$ to 8 [(a) to (h)]. The $\tilde{\gamma}^r_{Rc}$ for the two states $R = 1, 2$ with the largest widths are represented by dashed lines while the $\tilde{\gamma}^r_{Rc}$ for all the other states $R = 3, ..., 70$ are shown by points at the radii r for which the calculations are performed. The solid curves belong to a typical trapped state.

the short-lived states could be comparable to that of the long-lived states since they result from the interferences of all (overlapping) resonance states. The lifetimes of the states differ, however, so strongly from each other that one expects intuitively also differences in their radial distribution.

In a schematic example considered in [7], the short-lived states are concentrated at the surface what seems to be in contrast to the result obtained by us. In the example discussed in [7], a finite chain of potential wells is considered where only the outer wells are coupled to the exterior. In this system, the exit is possible from the surface only. Thus, the short-lived state is concentrated at the surface as a consequence of the way the potential is constructed. A similar result is expected if the calculations for nuclear reactions are performed with a surface δ interaction.

In our model calculations, no area of the nucleus is distinguished from the other ones from the very beginning. The residual interaction does not favor any specific value of the radius. All areas contribute in the same manner according to the assumptions of the model. Thus, there is no preassumption for the localization of the states coupled strongly to the continuum.

As one sees from Eq. (11), the radial dependence of $\tilde{\gamma}^r_{Rc}$ results from the interference of the bound and un-

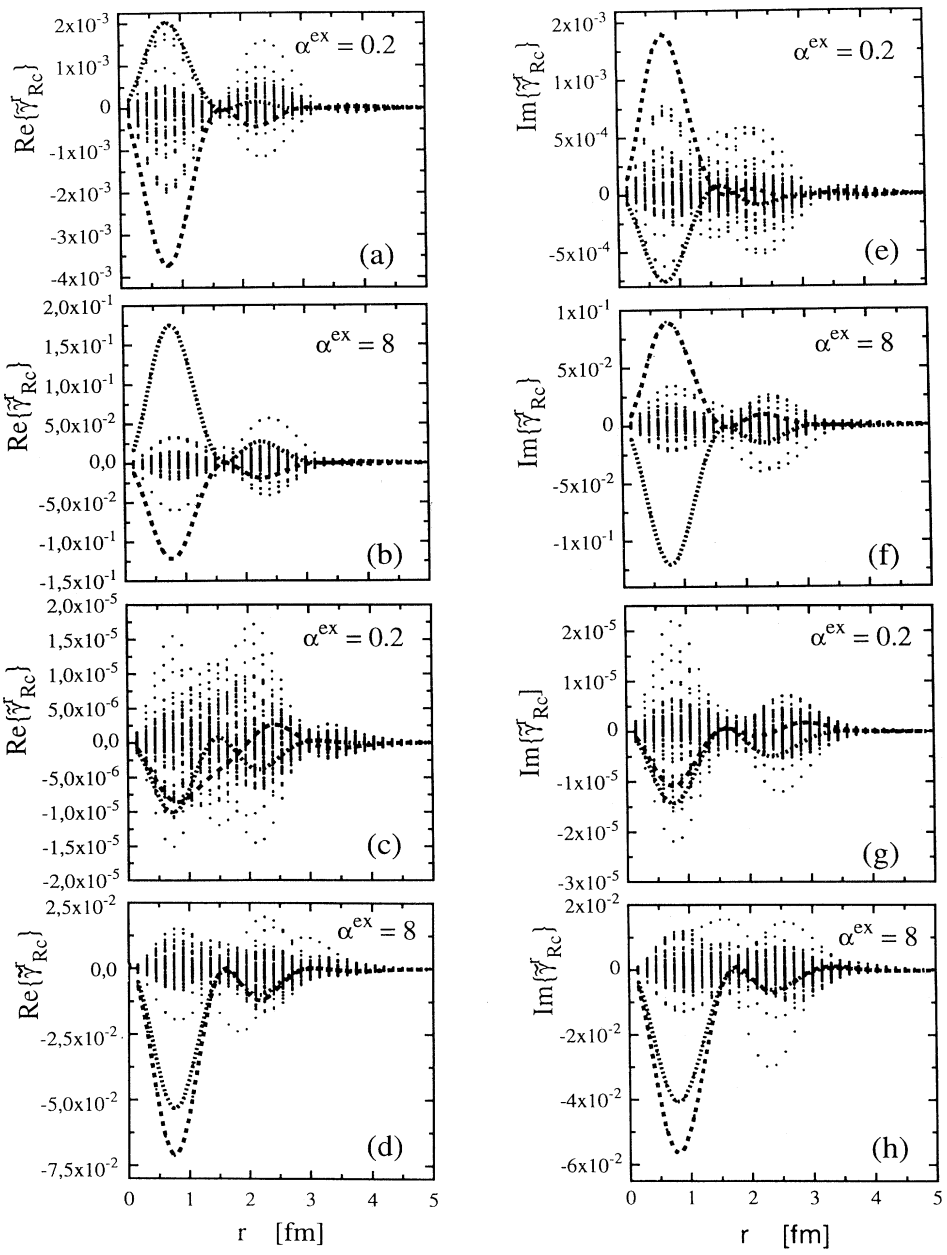

FIG. 2. Re$\{\tilde{\gamma}^r_{Rc}\}$ and Im$\{\tilde{\gamma}^r_{Rc}\}$ for the elastic channel c_1 (a,b,e,f) and the inelastic channel c_2 (c,d,g,h) in the case of proton decay. $\alpha^{ex} = 0.2$ and 8. The $\tilde{\gamma}^r_{Rc}$ for the two states $R = 1$, 2 with the largest widths are represented by dashed lines while the $\tilde{\gamma}^r_{Rc}$ of all the other states $R = 3, ..., 70$ are shown by points at the radii r for which the calculations are performed.

bound one-particle wave functions at the radius r. For illustration, in Figs. 3 and 4 the radial dependence of the one-particle wave functions is shown. The contribution of the d waves to the scattering wave functions $\xi^t_{j',E}$ at radii $r \leq 1$ fm (Fig. 3) is about zero. The amplitude of the scattering wave functions at these small radii is determined therefore by the s waves. The amplitudes of the bound s waves at $r \leq 1$ are larger than the amplitudes of the bound p and d waves (Fig. 4). We conclude from these results that the peak near 0.8 fm in $\tilde{\gamma}^r_{Rc}$ of the short-lived states is caused, mainly, by the constructive interference of bound and unbound one-particle s waves.

At larger radii, the contributions from the higher l waves cannot be neglected. Destructive interferences of the different waves may play, therefore, an important role.

The results obtained in the present paper suggest that the redistribution taking place in the nucleus in the neighborhood of the critical value α^{ex}_{cr} creates *structures in space and time by self-organization.* This statement will be explained in the following.

According to the general understanding, self-organization occurring in open systems leads to the creation of states with a high degree of order. A measure for the degree of order of a system is its entropy. Haken [20] used successfully the conception of the information (or Shannon) entropy in order to characterize the formation of high-ordered states by self-organization at a certain

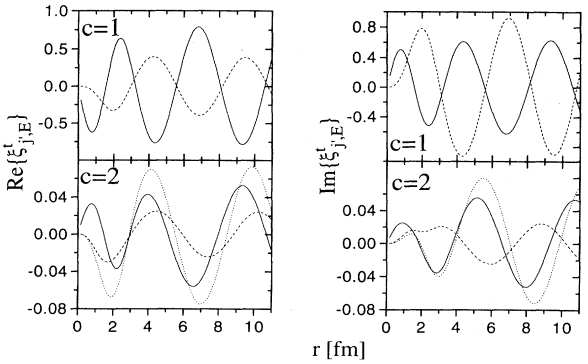

FIG. 3. Real (a) and imaginary (b) parts of the scattering wave functions $\xi^t_{j',E}(r)$ for s waves (full lines), $d_{3/2}$ waves (dashed lines), and $d_{5/2}$ waves (dotted lines) versus the radius r relative to the ground state (c=1) and first excited state (c=2) of ^{15}O.

critical value of a so-called control parameter.

In our calculations, the parameter α^{ex} plays the role of a control parameter [12]. It simulates the degree of overlapping of the resonances, i.e., the interaction of the resonances via the continuum of decay channels. The information entropy of the system as a function of α^{ex} is investigated in [12]. As a result, the information entropy of *all* modes, including the relevant and irrelevant ones, increases with increasing α^{ex}. The information entropy of the relevant modes (short-lived states at $\alpha^{ex} > \alpha^{ex}_{cr}$) alone is, however, smaller than the information entropy of the whole system at values $\alpha^{ex} \simeq \alpha^{ex}_{cr}$. The main part of the information entropy at $\alpha^{ex} > \alpha^{ex}_{cr}$ is in the many long-lived states. The existence of these long-lived states allows to fix the energy to an accuracy much higher than the energy uncertainty characteristic of the system which is determined by the collision time of the constituent particles. The long-lived states are, therefore, *not* relevant for the system at time and energy scales characteristic of it (although they may be identified in high-resolution experiments and are decisive in the long-time scale).

Beyond the critical region of the control parameter, the main part of the information entropy is, therefore, in irrelevant modes. This result is in agreement with the results obtained and discussed by Haken [20]. The reduction of the information entropy of the system (which should be identified with the relevant modes) takes place by means of the formation of irrelevant modes which carry a large amount of information entropy. Altogether, there is no contradiction to the second law of thermodynamics [20].

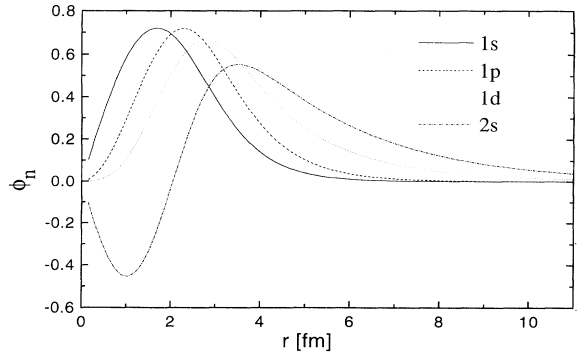

FIG. 4. The different bound one-particle wave functions $\phi_i(r)$ versus the radius r.

In other investigations on self-organization (e.g., [21]), the entropy is divided into two parts, $S = S^{in} + S^{ex}$, where S^{in} is the entropy of the system and S^{ex} denotes the entropy of the environment. It is supposed that S^{in} decreases as a result of self-organization but S^{ex} increases so that the sum S of both parts does not decrease, $\delta S \geq 0$, in agreement with the second law. In these investigations, the formation of highly-ordered structures is accompanied by an "export" of entropy into the environment.

There is a long discussion in the literature on the differences of these two entropy considerations in self-organizing systems (e.g., [20]). In any case, self-organization is nothing else than the reduction of the number of relevant degrees of freedom which occurs under certain "critical" conditions by means of the interaction of the system with its environment. That means, the system before and after the reorganization is not the same (when we identify the system with the relevant modes). The number of degrees of freedom of the system is large as long as the control parameter is below its critical value, while this number is effectively reduced by formation of a few relevant modes at values of the control parameter beyond its critical point.

The results of our calculations show that both entropy considerations are *not* in contradiction with each other in the case of our model investigations. The short-lived states which are relevant at time and energy scales characteristic of the system and $\alpha^{ex} > \alpha^{ex}_{cr}$, are localized at small radii in contrast to the long-lived states which are spread over a large radial extension. In other words: the system forms *structures in space*. The corresponding information entropy is small [12]. The results of our calculations show further that the entropy export takes place by formation of modes in the critical region $\alpha^{ex} \approx \alpha^{ex}_{cr}$ which are irrelevant at time and energy scales characteristic of the system.

It is worth noting that such a consideration corresponds qualitatively to the (phenomenological) models used for the description of nuclei at low and at high level density. At *low* level density, the environment consists of the decay channels what is expressed by $\Gamma = \Gamma^{\uparrow}$ where $\Gamma^{\uparrow}$ is the escape width of a state (particle decay into the continuum). At *high* level density, however, the states coupled strongly to the decay channels, are supposed to decay into the continuum as well as into the compound nucleus states, $\Gamma = \Gamma^{\uparrow} + \Gamma^{\downarrow}$ where $\Gamma^{\downarrow}$ denotes the spreading width for the "decay" of the short-lived states into the long-lived compound nucleus states. An example are the isobaric analogue resonances the structure of which is described well by "parent nucleus + proton."

The results obtained by us show further that the *structures in space* which are formed at the critical point of the control parameter α^{ex} are short-lived. The corresponding time scale is well separated from the time scale of the long-lived states. The separation of these two time scales

as a function of α^{ex} can be traced by means of the results presented in Table I ("trapping effect").

Short-lived states may be considered as states with a small "extension" in the time, i.e., they may be identified with *structures in time* in analogy to the *structures in space* discussed above. Taking into account the trapping effect as well as the results shown in Figs. 1 and 2, the system consisting of the relevant modes at high level density ($\alpha^{ex} > \alpha_{cr}^{ex}$) can be identified therefore with a *structure in space and time*. It is formed by self-organization under the influence of the coupling to the continuum of decay channels.

The reorganization taking place at a certain critical value of the control paramenter α^{ex} in the open quantum mechanical system considered by us, may be viewed as an example for the processes happening in open quantum systems. They support the assumption by Prigogine (e.g., [15]) that *structures in space and time* are formed by self-organization.

V. SUMMARY

Summarizing, we conclude from our results on decaying states that there exists a correlation between the lifetimes of the states and their radial extensions. In the short-time scale, most nucleons are emitted from the regions of small radii. The nucleons emitted from the surface region of the nucleus appear mainly in the long-time scale. That means, we observe a correlation of the decay probability of nuclear states with their radial extension. The shorter the lifetime of a state, the smaller is its radius.

The results of our calculations support, therefore, the assumption that the trapping effect creates "structures in space and time." In this manner, the trapping effect may be considered as a signature for self-organization in the nuclear system.

ACKNOWLEDGMENTS

The present investigations are supported by the Deutsche Forschungsgemeinschaft (Ro 922/1) and by the Bundesministerium für Forschung und Technologie (WTZ X081.39).

[1] P. Kleinwächter and I. Rotter, Phys. Rev. C **32**, 1742 (1985); I. Rotter, J. Phys. G **12**, 1407 (1986); **14**, 857 (1988); Fortschr. Phys. **36**, 781 (1988).
[2] V.V. Sokolov and V.G. Zelevinsky, Phys. Lett. B **202**, 10 (1988); Nucl. Phys. **A504**, 562 (1989).
[3] V.B. Pavlov-Verevkin, Phys. Lett. A **129**, 168 (1988); F. Remacle, M. Munster, V.B. Pavlov-Verevkin, and M. Desouter-Lecomte, *ibid.* **145**, 265 (1990).
[4] I. Rotter, Rep. Prog. Phys. **54**, 635 (1991), and references therein.
[5] F.M. Dittes, I. Rotter, and T.H. Seligman, Phys. Lett. A **158**, 14 (1991).
[6] F.M. Dittes, H.L. Harney, and I. Rotter, Phys. Lett. A **153**, 451 (1991).
[7] V.V. Sokolov and V.G. Zelevinsky, Ann. Phys. (N.Y.) **216**, 323 (1992), and references therein.
[8] F. Haake, F. Izrailev, N. Lehmann, D. Saher, and H.J. Sommers, Z. Phys. B **88**, 359 (1992).
[9] R.D. Herzberg, P. von Brentano, and I. Rotter, Nucl. Phys. **A556**, 107 (1993).
[10] W. Iskra, I. Rotter, and F.M. Dittes, Phys. Rev. C **47**, 1086 (1993)
[11] K. Someda, H. Nakamura, and F.H. Mies, Prog. Theor. Phys. Suppl. **116**, 443 (1994).
[12] W. Iskra, M. Müller, and I. Rotter, J. Phys. G **19**, 2045 (1993); **20**, 775 (1994).
[13] P.A. Moldauer, Phys. Rev. Lett. **18**, 249 (1967).
[14] N. Bohr, Nature **137**, 344 (1936).
[15] I. Prigogine, *From Being to Becoming* (Freeman, San-Francisco, 1979).
[16] W. Iskra and I. Rotter, Phys. Rev. C **44**, 721 (1991).
[17] H.W. Barz, I. Rotter, and J. Höhn, Nucl. Phys. **A275**, 111 (1977).
[18] C. Mahaux and H.A. Weidenmüller, *Shell Model Approach to Nuclear Reactions* (North-Holland, Amsterdam, 1969).
[19] I. Rotter, Ann. Phys. (Leipzig) **38**, 221 (1981).
[20] H. Haken, *Information and Selforganization* (Springer, Berlin, 1988).
[21] W. Ebeling and R. Feistel, *Physik der Selbstorganisation und Evolution* (Akademie-Verlag, Berlin, 1986).